PHYSICAL REVIEW B, VOLUME 65, 033314

Symmetry-forbidden Raman scattering from porous silicon quantum dots

Md. N. Islam, R. N. Panda, A. Pradhan, and Satyendra Kumar
Department of Physics, Indian Institute of Technology Kanpur, Kanpur-208 016, India
(Received August 21 2001; published 2 January 2002)

We report on the observation of symmetry-forbidden Raman (SFR) scattering modes from porous silicon structures at room temperature. The intensity of SFR lines is significantly enhanced by optimizing the thickness of porous silicon layers attached to the c-Si substrates. X-ray diffraction analysis and scanning electron microscopy provided significant information on the structural orientation of PS layer to understand the symmetry violations in the Raman selection rules. A combination of various mechanisms such as crystallite size effects, lattice mismatch induced micromisorientations of crystal planes, and multiple reflections and refraction within the porous silicon nanostructures explains our results.

DOI: 10.1103/PhysRevB.65.033314 PACS number(s): 78.30.−j, 78.67.−n, 78.66.Jg, 63.22.+m

Ease of formation of electrochemically anodized porous silicon (PS) has proliferated the studies of quantum size effects in nanocrystalline silicon structures.[1] Small crystallite sizes in the range of few nanometers lead to three-dimensional confinement of electrons and holes as well as phonons. Raman scattering (RS) being sensitive to crystal potential fluctuations and local atomic arrangements, provides useful information on crystal symmetry and size effects. In the back scattering Raman configuration, the first order RS from the (100) surface of c-Si represents scattering by LO phonons having momentum $\mathbf{q}=0$ at Brillouin zone (BZ) center. All other features are normally forbidden and hence their intensities are very weak.[2] However, other acoustic or optical phonons may be observed in the Raman spectra due to violation of symmetry rules and /or from multiphonon processes under certain experimental conditions.[3] On the other hand, PS layers comprise of nanocrystallites with interconnecting micropores.[1] Consequently, PS lattice does not possess infinite translation symmetry, leading to relaxation of momentum conservation at BZ center. The phonons with momentum away from BZ center (i.e., $\mathbf{q}\neq 0$), decided by the crystallite size, are allowed to contribute to the first order RS.[4] RS profiles from Si nanostructures have been explained by phonon confinement effects in crystallites.[5–7] The effect of symmetry relaxation on the first-order optical phonon RS has been widely used to characterize the nanocrystalline size effects in PS.[8–13]

Recently, attention has been paid to the Raman scattering from higher order multiphonon effects[14,15] or acoustic phonons[16] due to the size confinement effects in Si. However, despite the fact that PS offers exciting possibilities of symmetry breaking due to its microstructure, very few authors have reported on phonon modes other than optical phonons in PS layers.[14,17] Tanino *et al.*[14] reported weak symmetry-forbidden Raman (SFR) modes only at low temperature (10 K) from *free standing* PS layers. We carried out a detailed study of symmetry-forbidden Raman scattering modes in the first-order RS on PS layers attached to the c-Si substrates. We report on the enhancement of SFR modes at room-temperature under commonly used backscattering configuration. X-ray diffractometry (XRD) is employed to understand the structural variations in PS layers leading to symmetry violations of Raman selection rules.

PS layers were prepared by electrochemically anodizing boron doped (100) single crystal Si wafers (~500 μm thick) of 6–10 Ω cm resistivity in a Teflon cell using HF (40–48 wt. %) and C_2H_5OH (99.9%) (1:1 by volume). A current density of ~10 mA cm^{-2} was used for anodization times varying from few minutes to several hours. A tungsten halogen lamp (50 W and 12 V) at a distance of 20 cm was used for white light illumination during anodization. Sample microstructure and thickness were determined using scanning electron microscopy (SEM). CuK_α and CrK_α lines were used for x-ray diffraction (XRD) in standard powder geometry. Unpolarized photoluminescence (PL) and RS from the *same* sampling spot were measured in back scattering configuration at room temperature in a Spex micro-Raman setup using the 514.5 nm line from Ar^+ laser source. Laser power was optimized to minimize laser induced heating effects on RS profiles. The diameter of the microprobe beam on the sample was ~3 μm. All samples reported in this study showed room temperature PL.[13]

Figure 1 shows room-temperature Raman spectra obtained from c-Si substrate and a PS layer (~50 μm thick on c-Si). In the unpolished (100) silicon substrate, a strong and sharp LO phonon line at ~521 cm^{-1} is present. In addition to this main peak, two very weak phonon frequencies are also seen in the RS profile from c-Si on a magnification of 40 times. These RS lines are centered at ~305 and 635 cm^{-1} having relative intensity ratios of 1.1×10^{-2} and 5.5×10^{-3} to the main Raman peak. These peaks are assigned to surface assisted 2TA (X) and LO+TA phonon modes, respectively.[18,19] These peaks are hardly observable on the polished side. On the other hand, we see several Raman peaks in the measured RS profile from the anodized porous silicon. For clarity, the measured spectrum is amplified only 1.4 times and various peaks have been deconvoluted using Gaussian line shapes in Fig. 1(b). The main LO Raman line in anodized PS sample is broadened and shifted towards lower frequencies. It can be decomposed into two peaks occurring at 514.4 and 497.5 cm^{-1}, having full width at half maximum (FWHM) of 18.5 and 62 cm^{-1}, respectively. Such features in RS from PS are the characteristics of nanocrystalline nature and have been understood in terms of phonon confinement effects.[5,6] The presence of asymmetric Raman intensity tail towards low frequencies in the main peak

 ©2002 The American Physical Society

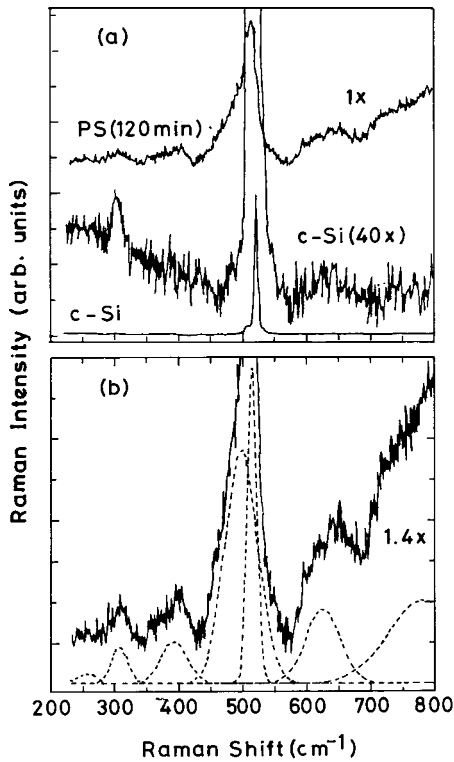

FIG. 1. Raman spectra from unpolished c-Si and porous Si layers measured at room temperature. The Gaussian deconvolution of various Raman peaks are shown as dotted lines (b).

(manifested by a peak at 497.5 cm^{-1} in deconvolution) may make one to believe that an amorphous Si phase exists in the PS structure. This actually may not be the case as discussed later. In fact, it has been found that a broad and asymmetric Raman peak in PS is a signature of crystallite size distribution in PS.[13] Anodized PS samples consist of a bimodal crystallite size distribution with smaller crystallites leading to quantum confinement effects reflected in RS and PL spectroscopies.[10,13] Considering a Gaussian size distribution in crystallite sizes, our analysis reveals a mean crystallite size $L_0 = 3.5$ nm with a standard deviation $\sigma = 0.76$ nm for this sample. Figure 1(b) also shows the enhanced relative intensities of RS lines at ~307 and 625 cm^{-1} as compared to the c-Si case. Furthermore, the RS profile from the PS layer contains new features at ~256, 392, and 780 cm^{-1}. In the present experimental configuration, only LO phonon modes are allowed and all other phonon modes are symmetry forbidden.

The microstructural effects can be strongly influenced by varying the layer thickness (anodization times) of PS. The Raman spectra on several PS layers are illustrated in Fig. 2. All spectra were measured under identical conditions (laser power, substrate temperature, etc.) and intensity of main LO peak was normalized. The intensity of SFR peaks relative to the main LO peak increases with increasing anodization times. However, for very long anodization times (>240 min) when thickness of the PS layer becomes comparable to the substrate thickness, the intensity starts decreasing. The relative intensities of SFR lines as compared to the main LO peak are strong in ~90 μm thick PS layer [spectrum (e) in Fig. 2]. The arrow marks on the upper X axis of Fig. 2 show the positions of dominant SFR lines. Based on experimental observations and theoretical calculations,[14,18–20] the assignments of various peaks to the acoustic and optical phonons are also marked in Fig. 2. Phonon dispersion curves provided by Tubino *et al.*[19] show that the effect of reduction in crystallite sizes (i.e., moving away from $\mathbf{q} = 0$) would be opposite on the shifts in optical and acoustic phonon frequencies. While optical phonon frequencies shift towards lower wave numbers on decrease in crystal size, they should increase for acoustic phonons. Further, presence of compressive strains is expected to increase the optical phonon frequencies and decrease the same for acoustic phonons.[18] Therefore, exact assignment of various SFR lines observed in PS is difficult.

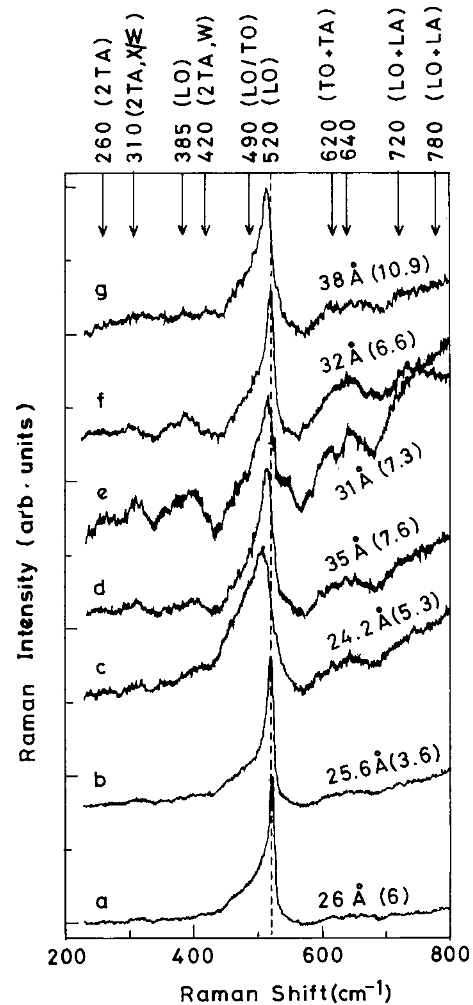

FIG. 2. Room-temperature Raman spectra from various porous Si layers grown at different anodization times, and having different film thicknesses: (a) 10 min, 5 μm; (b) 30 min, 10 μm; (c) 60 min, 30 μm; (d) 120 min, 50 μm; (e) 240 min, 90 μm; (f) 420 min, 150 μm; and (g) 600 min; 200 μm. The mean crystallite sizes and standard deviations (in brackets) deduced from the LO Raman peaks using a Gaussian size distribution (Ref. 13) are also shown.

Feng *et al.*[11] have observed acoustic phonons RS lines at around 300 and 600 cm^{-1} at 80 K. Tanino *et al.*[14] studied multiphonon modes from free standing PS samples at 10 K. These features of multiphonon Raman scattering in PS have

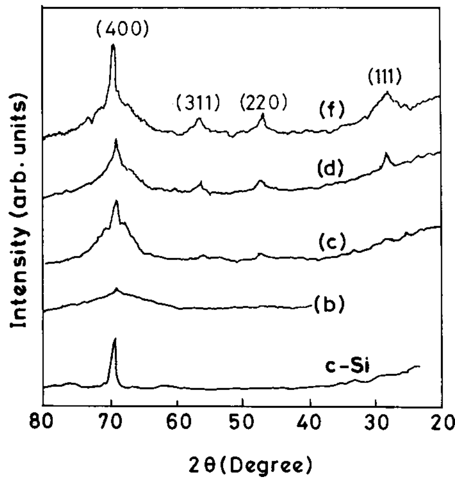

FIG. 3. The x-ray diffraction patterns from c-Si substrate and porous Si layers having different film thicknesses corresponding to samples shown in Fig. 2.

been attributed to relaxation of symmetry rules and surface assisted phonon scattering. Munder *et al.*[10] reported such a symmetry violation using a special 100(010,010)100 scattering configuration. They observed SFR lines towards higher frequencies, which have been attributed to the finiteness of the nanocrystallites and termed as surface-assisted multiphonon processes in PS.

The presence of enhanced SFR lines from PS layers at room temperature is clearly established (Figs. 1 and 2). To understand the origin of these SFR lines and probe the role of microstructural inhomogeneities, we carried out XRD measurements on the samples corresponding to Fig. 2. XRD spectra obtained using CuK_α radiation are shown in Fig. 3. As expected, the c-Si shows a sharp characteristic (400) x-ray peak at $2\theta = 69.2°$ which corresponds to the lattice constant $a = 5.43$ Å. In contrast, XRD from PS layers show broad and weak peaks corresponding to (400) plane. XRD patterns from PS do not indicate any features associated with amorphous silicon, which shows a broad diffuse scattering at around 28°. Interestingly for thick PS samples, peaks corresponding to (111), (220), and (311) Si planes also appear in the diffraction spectra [e.g., see curve (f) in Fig. 3]. These peaks could arise due to randomly oriented nanocrystallites in the thicker PS layers. Misoriented columns would also contribute to the XRD spectra. Further, (400) peak in thick PS layers consist of a diffused broad scattering base due to the nanocrystallites and a relatively sharp peak corresponding to (400) oriented silicon skeleton having larger grain sizes. The average crystallite sizes were determined from FWHM of diffused peaks using Debye-Sherrer formula and match well with those determined from Raman analysis (Fig. 2).

An expansion of porous silicon lattice has been seen using double crystal x-ray diffractometer.[21] It is difficult to observe the two separate XRD peaks corresponding to PS and c-Si in powder diffractometer, because of very high broadening of the PS peak (Fig. 3). However, in an appropriately designed XRD experiment, it may be possible to observe the separate x-ray peaks due to c-Si substrate and strained PS layer. We indeed observed such a clear split in XRD peaks using CrK_α radiation for relatively thinner ($\sim$10–15 μm) PS layers.[22]

Based on the XRD measurements, lattice strain up to $\sim$0.4% was estimated for different PS samples. The lattice dilation obtained from splitting of (400) XRD peaks is found to be larger by $\sim$50% compared to that for an identical powdered PS samples.[22] For symmetric biaxial stain ($\varepsilon_=$) parallel to c-Si/PS interface and neglecting shearing strains, the lattice dilation in perpendicular direction can be given as $\varepsilon_\perp = \varepsilon_=(1+2\nu)$, where ν is the Poisson's ratio.[21] From the measured values of $\varepsilon_\perp$ and $\varepsilon_=$, the value of ν is estimated to be varying from 0.05 to 0.25, which is relatively large as compared to the reported values.[21] The larger value of ν indicates the existence of asymmetry in lattice strain. This may be explained by considering the origin of lattice dilation in small crystallites. It is believed that lattice dilation in crystallites is caused by the distortion of surface atoms due to oxide and/or various add-atoms coverage.[23,24]

Raman peaks at around 300 and 380 cm^{-1} are observed in a-Si also and have been attributed to LA and LO phonon modes, respectively.[25,26] However, combining our x-ray and Raman TO mode analysis, the presence of significant amount of a-Si giving rise to enhanced SFR lines is ruled out. Furthermore, low frequency RS signal from oxidized PS is found to be much less compared to that from oxide removed PS after a brief dip in diluted HF.[10] Therefore assumption of a-Si and/or oxygen induced surface disorder in PS layers cannot account for the observed enhancement of SFR scattering from PS layers.

There could be a combination of effects giving rise to enhanced SFR scattering from PS layers. For example, size effects, anisotropic strains in the PS layers attached to the substrates, misorientations of the PS, and randomly oriented PS nanoparticles could all lead to the symmetry violations in the Raman selection rules. Bond polarizability model calculation of RS from nanocrystallites gives rise to lower frequency RS lines for smaller crystallites.[27,28] The intensity of these lines increase gradually as the crystallite size decreases. With increase in anodization time, the porosity increases and relative proportion of smaller crystallites increases. Further, our XRD data have shown the presence of strain at PS/c-Si interface. However, such a lattice distortion would not be present in free standing PS layers.[10,15] This could explain relatively weak multiphonon RS lines from free standing PS samples even at low temperatures.

In addition, with increasing anodization time, the thicker PS columns would enhance the multiple reflections and refractions (MRR) of the probe beam. This in turn, would increase the effects of misorientations. On the other hand, as one moves away from the PS/substrate interface the strain caused by lattice mismatch relaxes. As the incident laser beam has limited penetration depth, SFR intensities would decrease. The reverse is true for the effects of MRR. Therefore there will be compensatory effects of lattice strain and MRR in enhancing the SFR lines from thick PS layer attached to substrate Si. Indeed, the relative intensities of SFR lines in Fig. 2 go through a maximum for sample (e) and then decrease with further increase in anodization time. It

may be mentioned here that the PL intensity profiles versus anodization time also follow the same behavior as SFR lines (results not shown).

We have studied symmetry-forbidden Raman modes from PS layers grown on c-Si (100) substrate. Systematic micro-Raman study on PS layers prepared under different preparation conditions and anodization times has been carried out to enhance the intensity of SFR modes. The presence of neither amorphous silicon nor oxidation induced surface disorder can account for our results. A combination of mechanisms such as crystallite size effects, lattice mismatch induced micromisorientations of crystal planes, and multiple reflections and refraction within the PS nanostructures explains the strong SFR lines from porous silicon. Our explanation of observed behavior of SFR modes is supported by a careful x-ray diffraction analysis on the same samples.

[1] A. G. Cullis, L. T. Canham, and P. D. J. Calcott, J. Appl. Phys. **82**, 909 (1997).

[2] M. Cardona and G. Guntherodt, *Light Scattering in Solids II* (Springer-Verlag, New York, 1982), Vol. 50, p. 49.

[3] E. Anastassakis and Y. S. Raptis, J. Appl. Phys. **57**, 920 (1985).

[4] See for example, M. Kitajima, Crit. Rev. Solid State Mater. Sci. **22**, 275 (1997).

[5] H. Richter, Z. P. Wang, and L. Ley, Solid State Commun. **39**, 625 (1981).

[6] I. H. Campbell and P. M. Fauchet, Solid State Commun. **58**, 739 (1986).

[7] S. Veprek, F. A. Sarott, and Z. Iqbal, Phys. Rev. B **36**, 3344 (1987).

[8] R. Tsu, H. Shen, and M. Dutta, Appl. Phys. Lett. **60**, 112 (1992).

[9] Z. Sui, P. P. Leong, I. P. Herman, G. S. Higashi, and H. Temkin, Appl. Phys. Lett. **60**, 2086 (1992).

[10] H. Munder, C. Andrezjak, M. G. Berger, U. Klemradt, H. Luth, R. Herino, and M. Ligeon, Thin Solid Films **221**, 27 (1992).

[11] Z. C. Feng, J. R. Payne, and B. C. Covington, Solid State Commun. **87**, 131 (1993).

[12] A. Roy, K. Jayaram, and A. K. Sood, Solid State Commun. **89**, 229 (1994).

[13] Md. N. Islam and Satyendra Kumar, Appl. Phys. Lett. **78**, 715 (2001).

[14] H. Tanino, A. Kuprin, H. Deai, and N. Koshida, Phys. Rev. B **53**, 1937 (1996).

[15] R. Wang, G. Zhou, Y. Liu, S. Pan, H. Zhang, D. Yu, and Z. Zhang, Phys. Rev. B **61**, 16 827 (2000).

[16] M. Fujii, Y. Kanzawa, S. Hayashi, and K. Yamamoto, Phys. Rev. B **54**, R8373 (1996).

[17] J. C. Tsang, M. A. Tischler, and R. T. Collins, Appl. Phys. Lett. **60**, 2279 (1992).

[18] B. A. Weinstein and G. J. Piermarini, Phys. Rev. B **12**, 1172 (1975).

[19] R. Tubino, L. Piseri, and G. Zerbi, J. Chem. Phys. **56**, 1022 (1972).

[20] P. A. Temple and C. E. Hathaway, Phys. Rev. B **7**, 3685 (1973).

[21] K. Barla, G. Bomchil, R. Herino, J. C. Pfister, and J. Baruchel, J. Cryst. Growth **68**, 721 (1984).

[22] Md. N. Islam and Satyendra Kumar (unpublished).

[23] Z. Iqbal and S. Veprek, J. Phys. C **15**, 377 (1982).

[24] T. Ito, H. Kiyama, T. Yasumatsu, H. Watanabe, and A. Hiraki, Physica B **170**, 535 (1991).

[25] M. H. Brodsky, M. Cardona, and J. J. Cuomo, Phys. Rev. B **16**, 3556 (1977).

[26] A. A. Sirenko, J. R. Fox, I. A. Akimov, X. X. Xi, S. Ruvimov, and Z. Liliental-Weber, Solid State Commun. **113**, 553 (2000).

[27] P. A. M. Rodrigues, H. A. Cerdeira, and F. Cerdeira, Int. J. Mod. Phys. B **3**, 1167 (1989).

[28] J. Zi, H. Buscher, C. Falter, W. Ludwig, K. Zhang, and X. Xie, Appl. Phys. Lett. **69**, 200 (1996).